On Three-Dimensionality of Turbulent Buoyant Channel Flow

Osama A. El-Samni *

Department of Mechanical Engineering, The University of Alexandria, El-Chatby, Alexandria 21544, Egypt

Abstract

A three-dimensional buoyancy-driven turbulent boundary layer is generated in fully developed turbulent channel flow. Setting the buoyancy forces perpendicular to the mean flow direction and using high Grashof number result in strong cross flow which is expected to have a similar influence to that of the previously studied pressure- and shear-driven three-dimensional turbulence boundary layers (3DTBLs). The present buoyancy-driven configuration has the advantage of being in equilibrium and three-dimensional from inception. Few issues are presented and discussed in order to give better understanding of the underlying physics associated with buoyancy-induced 3DTBL flows. The characteristics of the resulting 3DTBL are examined in comparisons with the available data in the literature. Reduction of the structure parameter A_1 (defined as the ratio between the total Reynolds shear stress to twice the turbulent kinetic energy TKE) is noticed in the edge of the inner layer which is attributed to the reduction of both Reynolds shear stress and turbulent kinetic energy. Explanation for such reductions is given by examining the changes in coherent structures due to buoyancy effect. Comparisons of some relevant quantities used in turbulence modeling with those of 2DTBL flow reveal the difficulty of establishing a universal model for a satisfactory 3DTBL flow prediction.

Keywords: Buoyancy; Channel flow; Turbulence; Direct numerical simulation; 3DTBL;

1. Introduction

Buoyancy forces play a significant role in various industrial equipment which deals with heat exchange. The effects of buoyancy should be taken into account in the optimum design of such equipment. One of the issues that has not been covered in detail is the flow three-dimensionality generated by buoyancy. In this specific case, the three-dimensionality takes place when the gravity vector is parallel to the duct walls (mainly in case of vertical walls) but perpendicular to the mean flow direction. Lateral motions are generated causing the flow to skew in the transversal direction. Consequently, all Reynolds shear stresses and heat flux components become non-zeros. The difficulty of dealing with 3DTBL flows arises from poor predictions of the flow velocities with the current turbulence models which in turn lead to poor predictions of the thermal field. Most of the commercial software packages dealing with thermal equipment design are using turbulence models based on 2DTBL assumption. There is still great need to assess and improve such turbulence models to deal with three-dimensional flows in general and more specifically with buoyant flows. Therefore, understanding the underlying physics of three-dimensional buoyant flow is essential before improving the relevant models.

3DTBL flows have been explored extensively in laboratories, to our knowledge, without imposing buoyancy forces. The three-dimensionality is likely to occur in a nominally 2D flow by imposing a cross-stream pressure gradient which skews the flow in the near-wall region more strongly than near the free stream direction. Different techniques have been used in pressure-driven flows experiments to generate a 3DTBL. Schwarz and Bradshaw [1-3] and Flack [4] used a flat end-wall of constant area rectangular duct including a 30° bend around its mid point. Bradshaw and Pontikos [5] simulated an infinite swept wing by a deformable roof of a duct and measurements were done on its flat floor. Ölçmen and Simpson [6] used a wing-body junction type which is mounted vertically on a flat wind-tunnel wall. Compton and Eaton [7], Anderson and Eaton [8], and Eaton [9] generated their 3DTBL by constructing upstream facing wedges of different angles. Skewing the flow can also be developed by shear force when a wall moves in a direction different from the main flow direction. An example of the shear-driven flows is the experiments of Littell and Eaton [10], Chiang and Eaton [11] and Kang et al. [12] of flow on a free rotating disk.

Direct numerical simulation (DNS) has become a vital tool in 3DTBL flows discovery. DNS can simulate 3DTBL cases which cannot be realized experimentally. For example, Spalart [13,14] simulated turbulent boundary layer on a flat plate. He showed that when the free-stream

---

* Corresponding author. e-mail: elsamni@gmail.com

velocity vector rotates at constant angular rate, the resulting mild skewing of the velocity in this configuration resembles turbulent Ekman layer [15]. Moin et al. [16] applied a spanwise pressure gradient in a 2D channel flow. Non-equilibrium simulations were done by Coleman et al. [17, 18] by imposing mean irrotational deformations in the streamwise-spanwise planes which can mimic a favorable or an adverse pressure gradient. Le et al. [19] imposed an impulse spanwise movement to the lower wall of a turbulent channel flow. Wu and Squires [20] used large eddy simulation to predict a three dimensional equilibrium boundary layer by rotating the free-stream velocity over an infinite plate which resembles the growth of TBL over a rotating disk.

The present study tries to give more insight to the three-dimensionality induced by buoyancy forces. Various structural parameters which are usually used in describing 3DTBL flows will be compared with those of pressure- and shear-driven 3DTBLs. Explanation for the reduction of the structure parameter A_1 will be given in terms of the changes of the near-wall coherent structures. Some modeling issues will be covered by comparing the relevant quantities with those of 2DTBL flows.
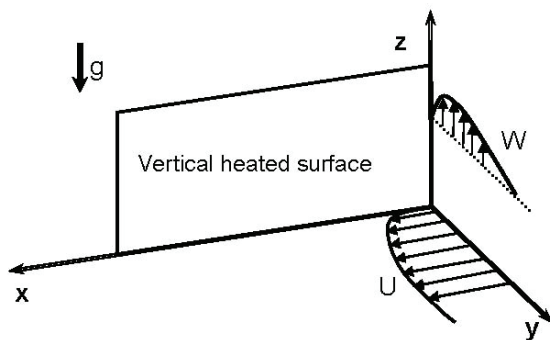

Fig. 1 Sketch of 3DTBL driven by buoyancy.

2. Numerical Approach

Vertical channel with two differentially heated walls are used for the present simulation in which the air flows horizontally and thus buoyancy vector is perpendicular to the mean flow direction. The focus will be on the heated wall as shown in.Figure .1. The temperature difference ΔT is sufficient to account for the buoyancy effect. The continuity, Navier-Stokes equations and the energy equation are solved using Pseudospectral code for a channel flow. It eliminates the pressure by transforming the Navier-Stokes equations to the vorticity-normal velocity formulation. Fourier series have been used for expanding the resolved variables in the homogenous directions while Chebyshev polynomial expansion is employed in the wall-normal direction. The driving pressure gradient is adjusted to keep constant mass flow rate in the x-direction. The channel width is 2δ and the computational domain has the dimensions $5\pi\delta \times 2\delta \times 2\pi\delta$ with grid points 128×129×128 in x, y, and z directions, respectively. The flow is assumed fully developed so that the periodic boundary conditions are applied in x and z-directions. The no-slip boundary conditions for the flow field and the isothermal boundary conditions with zero fluctuations are applied at both walls.

Further details about the numerical approach and the verification of the code can be found in El-Samni et al. [21]. The friction Reynolds number $Re_\tau = u_\tau \delta / \nu$ is fixed 164, where u_τ is friction velocity; d is half the channel depth and n is the kinematic viscosity. Grashof number, defined by $gb\Delta T(2d)^3/n^2$, is set to 4×10^6, where g is the gravitational acceleration and b is thermal expansion coefficient..

3. Results and Discussions

The present configuration is advantageous in terms of the simplified statistics compared with other 3DTBL flows. The equilibrium status of the flow and the homogeneity in the planes parallel to the stream wise-span wise directions make the quantities under consideration changing only in the wall-normal direction y. The quantities presented here are normalized by the friction velocity u_t^* deduced from the total mean velocity $Q = (U^2 + W^2)^{1/2}$ and n unless otherwise stated and are superscripted by $+$. Some quantities may be normalized by the momentum thickness q. Capital letters and over-bar denote the time and spatial average over $x - z$ planes and prime indicates the fluctuation component which may be dropped for clarity.

3.1. Polar Plot

With the above mentioned configuration, the buoyancy forces induce anti-symmetric mean span wise velocity (W) giving positive values near the heated wall as sketched in Figure .1

The peak of w occurs at $y^+ \sim 26$ which is smaller than those values observed in typical 3DTBL flows; see for example Wu and Squires [20]. Polar plot of the cross-flow velocity profile is shown in Fig. 2 where both the stream wise and span wise mean velocity components are normalized by the centerline velocity U_C.
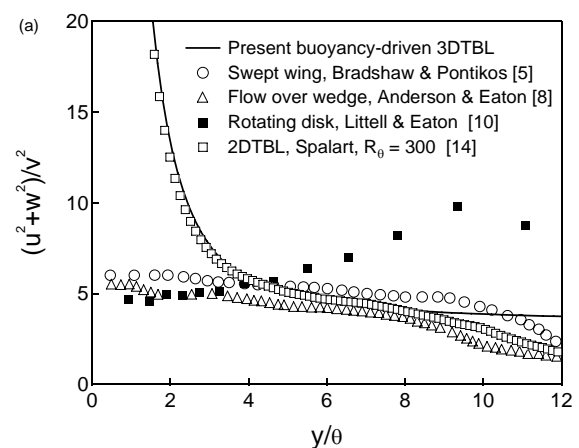

Fig. 2 Polar velocity.

The profile is compared with the 3DTBL data of the $30°$ bend [4] and the rotating disk [10] aiming at showing the relative magnitudes of the induced spanwise mean velocities in different 3DTBL flows. The apex of the

triangle reaches a maximum value of around 0.34. The peak value shown in the polar plot is larger than the value observed in the 30° bend of Flack [4] whose peak was around 0.25 and that of the rotating disk of Littell and Eaton [10] which approached 0.11. It can be noted also that the slope near the channel center is steeper than those observed in the experiments of 3TDBL in the outer layer. This difference in the profile shape and the peak of the polar plots can be attributed to the non-vanishing strain resulted from the anti-symmetric trend of W in the present study. In most of the 3DTBL flows, W in the outer layer vanishes resulting in very small $\partial W / \partial y$.

3.2. 3DTBL Structural Parameters

In this section, several structural parameters which are generally used in characterizing 3DTBLs are deduced from the statistical quantities presented in El-Samni et al. [21]. Of those parameters is the ratio of the wall-parallel normal stresses to the vertical normal stress, $(u'^2 + w'^2)/v'^2$ which can be a measure of the turbulence anisotropy. Comparisons with data of swept wing of Bradshaw and Pontikos [5], flow over wedge of Anderson and Eaton [8], rotating disk of Littell and Eaton [10], and Spalart [14] are presented in Fig. 3(a). Due to the continuity constraint at the wall, v is very small in the vicinity of the wall and consequently $(u'^2 + w'^2)/v'^2$ estimated from numerical simulation of Spalart [14] and the present simulation are two orders of magnitude larger than those of the experiments mentioned above. In the range $4 < y/\theta < 8$, the experiments of Littell and Eaton [10] and Bradshaw and Pontikos [5] show similar flatten profiles around the same value of the present study, between 3.8 ~ 5. At the outer edge of the boundary layer, $(u'^2 + w'^2)/v'^2$ approaches a value 2, the isotropic state for most of 3DTBL flows. However, in the present study it reveals a value around 3.6 showing high anisotropy in the core region due to the large increase of $w'w'$. Rotating disk [10] gives lower value of $(u'^2 + w'^2)/v'^2$ near the wall and increases in the far field with increasing the wall distance y. This trend is opposite to the present 3DTBL buoyant channel trend which starts very high at the wall and decreases with increasing y.

Another relevant parameter is the ratio of the wall-normal stress to the total shear stress magnitude $v'^2/[(u'v')^2 + (v'w')^2]^{1/2}$. The significance of this parameter was deduced from its trend in 2DTBL flows. In 2DTBL, $\overline{u'v'}$ is proportional to $\overline{v'^2}$. If such correlation exists in a 3DTBL flow, a simple relationship between the two quantities may reduce the number of unknowns in the turbulence model. In Fig. 3(b), a plateau profile in the range $50 < y^+ < 250$ can be noticed which resembles those of Spalart [14] and that of Compton and Eaton [7] but with higher values. In the inner layer, the profile is close to those of 2DTBL flows of Spalart [14]. However, in contrast to both Reynolds numbers of the 2DTBL of Spalart[14], this parameter does not show sharp increase in the outer layer due to the increased total shear stress $[(u'v')^2 + (v'w')^2]^{1/2}$ in the core region. The structure parameter A_1, defined by $[(u'v')^2 + (v'w')^2]^{1/2}/k$, has been

widely investigated in most of the previous 3DTBL flows. In general, three-dimensionality results in reduction of A_1 than its value in 2DTBL of around 0.15. In Fig. 3(c), A_1 is plotted in comparison with other numerical and experimental results. Reduction of A_1 at $y^+ < 120$ is observed in the present study in accordance with the reduction revealed in 2DTBL of Spalart [14] at $Re_q = 1410$, the bend flow of Flack [4], and the rotating disk of Wu and Squires [20] at $Re_t \sim 840$. However, at $y^+ > 120$, A_1 increases. Although turbulent kinetic energy increases in the outer layer, still A_1 reveals higher value which indicates the efficiency of the flow to generate shear stress in the core region of the channel. This can be attributed to the nearly constant mean strain dW/dy across the channel core in the present case.
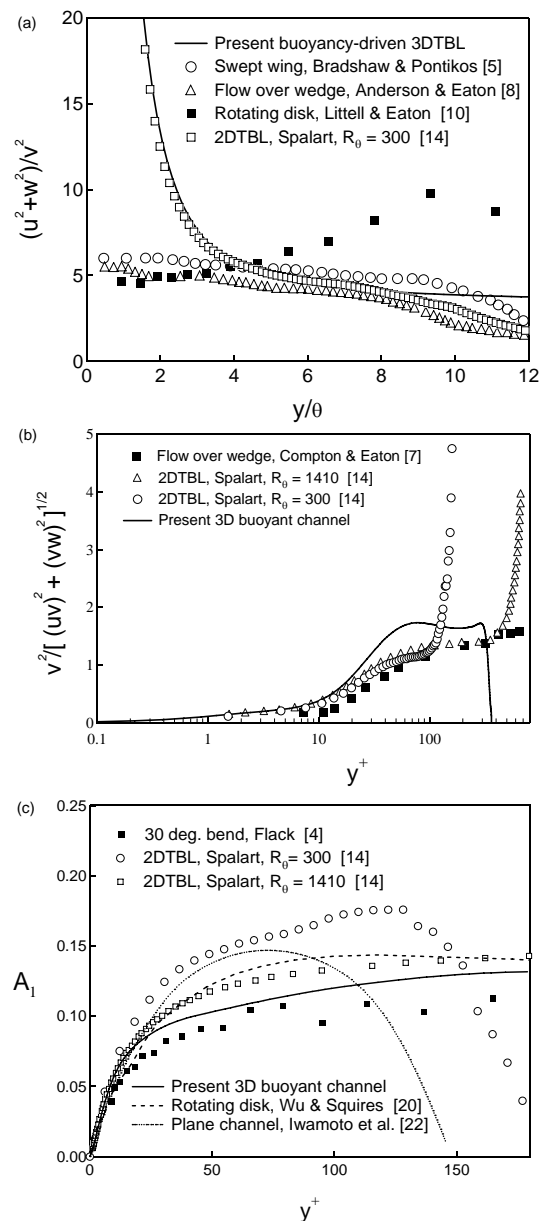
Fig. 3 Turbulence structures; (a) $(u'^2 + w'^2)/v'^2$; and (b) $v'^2/[(u'v')^2 + (v'w')^2]^{1/2}$; and (c) A_1.

The present 3DTBL buoyant flow resembles the rotating disk flow. Both are three-dimensional from inception and have their peaks of the spanwise velocity W in near-wall region. Although they show reduction of A_1, their anisotropy behaviors are different as shown in Fig. 3. This inconsistency, even between similar 3DTBL flows, reveals again the difficulty of proposing a universal discreption of 3DTBLs in the inner and outer regions.
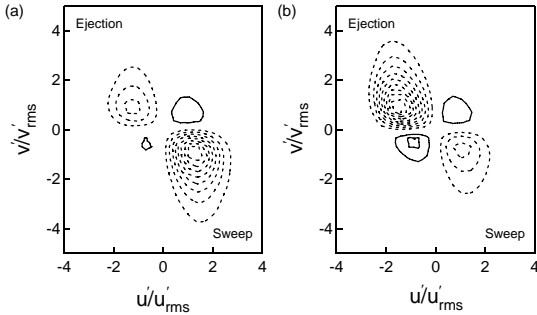

Fig. 4 JPDF of u' and v' at $y^+ \sim 12.5$: (a) weighted with positive w'_x ; (b) weighted with negative w'_x .

3.3. Changes of Coherent Structures

Several studies have tried to investigate the effects of three-dimensionality on the near-wall structures aiming at explaining the responsible mechanism of Reynolds shear stress reduction. Littell and Eaton[10], Kang et al.[12] and Wu and Squares[20] showed that cross flow reduces the ability of positive streamwise vortices to produce strong ejections ($u' < 0, v' > 0$) while weakening the ability of the negative ones to produce strong sweeps ($u' > 0, v' < 0$). In order to examine this hypothesis, the joint probability density function (JPDF) weighted by positive and negative streamwise vortices is performed and plotted in Fig. 4(a) and (b), respectively. This is performed at the height where both sweep and ejection events are of equal contribution to Reynolds shear stress $-\overline{u'v'}$ which is found to be at $y^+ \sim 12.5$. In 2DTBL case, the contours of the weighted JPDF are anti-symmetry in the diagonal connecting the 2nd and 4th quadrants. Clear agreement with the above claim can be seen in the Fig. 4 where positive w'_x is associated with weak ejections and negative w'_x is associated with weak sweeps. Two-point velocity correlation R_{uv} commonly defined by $R_{uv}(r_z) = \overline{u'(z)v'(z+r_z)}/u'_{rms}v'_{rms}$ is plotted in Fig. 5 at the same height of that used in Fig. 4. However, there exists a strong dip in the negative separation in agreement with Littell and Eaton[10] and Kang et al.[12]. This asymmetry of the correlation coefficient implies that the strength of positive and negative vortices is not statistically equivalent. In other words, if both kinds of vortices are weakened with the same degree, the correlation R_{uv} should be symmetry around $r_z = 0$.

Decomposition of RMS of ω'_x based on their signs can verify the difference of strength of each kind of vortices. Kim et al. [23] estimated roughly a measure for the size and strength of vortices based on the peaks location of

ω'_x. In Fig. 6(a), the positive vortices appear stronger than the negative ones since the later have weaker peak and the spacing between its local peaks becomes wider. Another verification is performed Fig. 6(b), where the number of events corresponding to $|w'_x| > 2 w'_{x,rms}$ is estimated for long time of integration. In 2DTBL, the number of positive and negative vortices exceeding any threshold should be identical as long as the two vortices are symmetry. However, it can be seen that at $y^+ \sim 20$ the positive ω'_x has a clear peak in the time that negative w'_x has a minimum. The location $y^+ \sim 20$ refers to the centers of vortices [23].
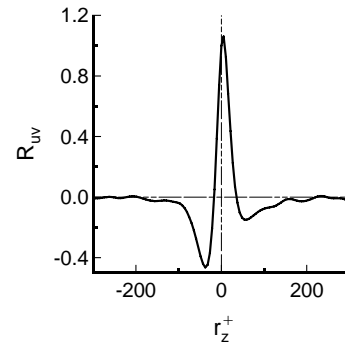

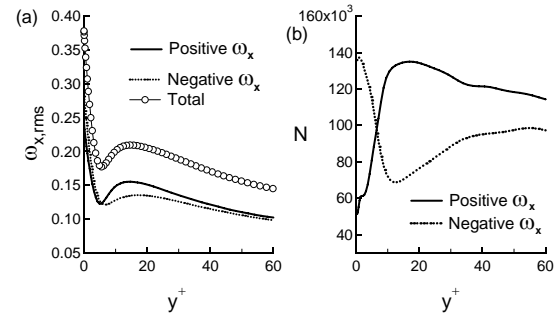Fig. 5 Correlation coefficient at $y^+ \sim 12.5$.

Fig. 6 (a) Vorticity decomposition; (b) number of strong vorticity RMS events

3.4. Modeling Issues

The above mentioned structural parameters are used in deriving various constants of the k-ε model. More derived quantities of interest to Reynolds-averaged modeling are computed in this section. It was shown by El-Samni et al. [21] that there is a lag between the shear stress and the mean velocity gradient vectors which makes restriction on using isotropy eddy viscosity assumption in turbulence modeling. A verification of their claim can be checked out by looking at the eddy-viscosity ε_x and ε_z in the stream wise and span wise directions:

$$\text{where } \varepsilon_x = \frac{-\overline{u'v'}}{\partial U/\partial y} \text{ and } \varepsilon_z = \frac{-\overline{v'w'}}{\partial W/\partial y}$$

In most of the 3DTBL flows studied so far, the eddy viscosity is not isotropic which means that $e_x \neq e_z$. This inequality has made unrealistic predictions of 3DTBL

flows using turbulence models based on the isotropy eddy-viscosity assumption. As shown in Fig. 7(a), ε_x matches with the 2DTBL values in near wall region while it departs substantially in the outer layer. ε_z oscillates from negative to positive at $y^+ \sim 26$ where the dW/dy changes its sign. Shown in Fig. 7(b) is the ratio $\varepsilon_x/\varepsilon_z$ which is denoted as the anisotropy factor N_e. Its value is far from unity in most of the channel depth in agreement with values obtained in other 3DTBL [6, 7].
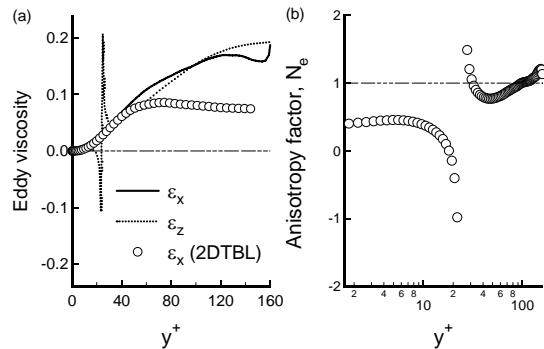

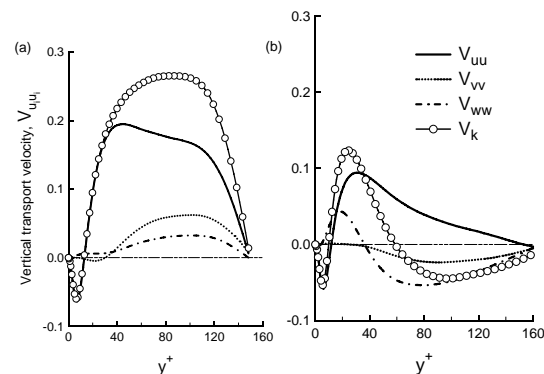Fig. 7 Eddy viscosity (a); the anisotropy factor Ne.

Fig. 8 Vertical transport velocities: (a) 2DTBL; (b) 3DTBL.

The effect of turbulence to transport turbulent kinetic energy can be expressed as an effective vertical transport velocity which is the sum of the three normal Reynolds stresses transport velocities:

$$V_k = (\overline{u'^2 v'} + \overline{v'^3} + \overline{w'^2 v'})/k$$

These triple correlations are commonly used in the transport equations of the normal Reynolds stresses. In near wall region, turbulent kinetic energy is transported away from the wall similar to 2D and 3DTBL flows as shown in **Fig. 8**(a,b). The major changes due to the buoyancy effect can be seen in the outer layer ($y^+ > 30$) in which V_k becomes negative in contrast to the 2DTBL profile and also to other 3DTBLs [1, 2, 5] and [8]. That is due to the change of transport direction of both V_{vv} and V_{ww} as shown in **Fig. 8**(b).

The triple products used in the closure of transport equations of Reynolds shear stresses $-u'v'$ and $-v'w'$ are shown in **Fig. 9**. The growth of $w'v'^2$ can be seen easily with comparable values to the primary triple product $u'v'^2$.

The appearance of local peaks in $u'v'^2$ indicates the necessity to adjust turbulence models dealing with local shear stress gradient rather than the local shear stress values.

Last issue to be addressed is the pressure-strain correlation which is responsible for redistributing TKE among the velocity components and its trace should vanish. As shown in **Fig. 10**, the energy is redistributed from u and v to w component in near-wall region of both 2D and 3DTBL but with larger contribution from v in the existence of buoyancy forces which enhance the eruption of plumes of hot fluid from the surface. In contrast to 2DTBL, the buoyancy modifies the redistribution of TKE in the outer layer so that the energy is redistributed from w to both u and v as shown in **Fig. 10**(b). Moin et al. [16] observed reduction of the pressure-strain due to the flow three-dimensionality in contrast to the present findings. This discrepancy reflects the difficulty to propose a reasonable assumption for the pressure strain term in turbulence models.
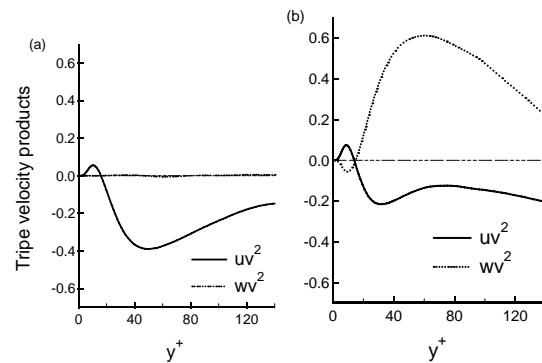

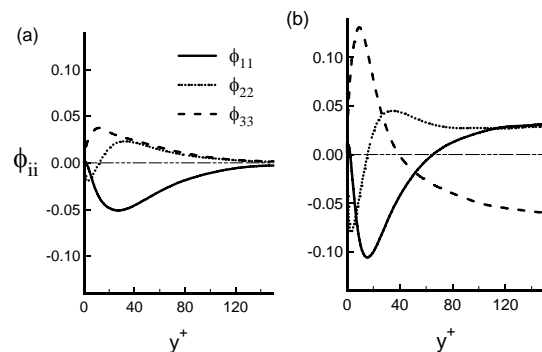Fig. 9 Triple velocity products: (a) 2DTBL; (b) 3DTBL.

Fig. 10 Pressure-strain correlation: (a) 2DTBL; (b) 3DTBL.

3.5 Practical Implementation

One of the practical applications of the present study is the drag reduction of turbulent flow. It was shown by Yoon et al. [24] that setting periodically arrayed heating and cooling strips in a vertical wall can lead to 11% drag reduction at the present studied Grashof number and 35% at Grashof number of 10^7. Such arrangements lead to reversing the directional effect of the buoyancy forces affecting the flow particles moving beside heated then cooled strips. Continuous reverse of the buoyancy forces leads to faster decay of both kinds of vortices and eventually to substantial drag reduction.

4. Conclusion

The present study demonstrates some of the 3DTBL features induced by buoyancy forces. The resulting 3DTBL flow is simpler than the previously investigated flows either experimentally or numerically since the relevant turbulent quantities are function only on the wall-normal direction. Moreover, the flow is three-dimensional from inception and therefore the transient and non-equilibrium effects are absent. The present configuration can be used repeatedly in testing and improving turbulence models. The significance of the present study lies in the predominance of the buoyancy forces in various thermal equipment and the necessity to provide deep understanding for the underlying physics in 3DTBL induced by buoyancy.

Comparisons with the previous experimental and numerical studies show that the present flow has similar characteristics with 3DTBL flows such as the reduction of the structural parameter A_1 . However, the anisotropy of the flow necessitates more concern about turbulence modeling dealing with flow three-dimensionality in addition to mixed convection. Intensive investigations on eddy viscosity models and full Reynolds stresses models are needed to test their closures. Difficulties of modeling the triple correlations and pressure-strain terms are presented.

Near-wall structures are proven to be asymmetry in accordance with various 3DTBLs flows. The ability of positive rotating vortices to produce ejection events is weakened; meanwhile, the ability of negative vortices to produce sweep motion is reduced. The resultant effect of both reductions is to reduce the total Reynolds shear stress in accordance with most of the previously studied 3DTBLs. The total contribution from events (ejections and sweeps) associated with the positively rotating vortices is larger than that of negatively rotating vortices.

Acknowledgments

References

[1] Schwarz, WR, Bradshaw, P., "Measurements in a pressure driven three-dimensional turbulent boundary layer during development and decay" AIAA J. Vol. 31, 1993, 1207-1214.

[2] Schwarz, WR, Bradshaw, P., "Turbulence structural changes for a three-dimensional turbulent boundary layer in a 30 degree bend". Journal of Fluid Mech. Vol. 272, 1994, 183-209.

[3] Schwarz, WR, Bradshaw, P., "Term-by-term tests of stress-transport turbulence models in a three-dimensional boundary layer" Phys. Fluids, Vol. 6, 1994, 986-998.

[4] Flack, KA. "Near-wall structure of three-dimensional turbulent boundary layers". Experiments in Fluids, Vol 3, 1997, 335-340.

[5] Bradshaw, P., Pontikos, NS, "Measurements in the turbulent boundary layer on an infinite swept wing" Journal Fluid Mech., Vol. 159, 1985, 105-130.

[6] Ölçmen, MS, Simpson, RL, "An experimental study of a three-dimensional pressure-driven turbulent boundary layer"J. Fluid Mech., Vol. 290, 1995, 225-262.

[7] Compton, DA, Eaton, JK, "Near-wall measurements in a three-dimensional turbulent boundary layer" Journal Fluid Mech., Vol. 350, 1997, 189-208.

[8] Anderson, SD, Eaton, JK," Reynolds stress development in pressure-driven three-dimensional turbulent boundary layers". J. Fluid Mech., Vol. 202, 1989, 263-294.

[9] Eaton, JK. "Effects of mean flow three-dimensionality on turbulent boundary layer structure". AIAA J., Vol. 33, 1995, 2020-2025.

[10] Littell, HS, Eaton, JK. "Turbulence characteristics of the boundary layer on a rotating disk.", J. Fluid Mech., Vol. 266, 1994, 175-207.

[11] Chiang, C., Eaton, JK. "An experimental study of the effects of three-dimensionality on the near wall turbulence structures using flow visualization" Experiments in Fluids, Vol. 20, 1996, 266-272.

[12] Kang, HS, Choi, H., Yoo, JY. "On the modification of the near-wall coherent structure in a three-dimensional turbulent boundary layer on a free rotating disk", Phys. Fluids, Vol. 10, 1998, 2315-2322.

[13] Spalart, PR. "Theoretical and numerical study of a three-dimensional turbulent boundary layer". J. Fluid Mech. Vol. 205, 1989, 319-340.

[14] Spalart, PR. "Direct simulation of a turbulent boundary layer up to $Re_q =1410$", J. Fluid Mech., Vol. 187, 1988, 61-98.

[15] Coleman, GN, Ferziger, JH, Spalart, PR. A numerical study of the turbulent Ekman layer. J. Fluid Mech., Vol. 213, 1990, 313-348.

[16] Moin, P., Shih, T.–H, Driver, D., Mansour, NN. "Direct numerical simulation of a three-dimensional boundary layer." Phys. Fluids , Vol. 2, 1990, 1846-1853.

[17] Coleman, GN, Kim, J., Spalart, PR." Direct numerical simulation of strained three-dimensional wall-bounded flows". Experimental Thermal Fluid Science , Vol. 13, 1996, 239-251.

[18] Coleman, GN, Kim, J., Le, A.-T. "A Numerical study of three-dimensional wall-bounded flows". Int. J. Heat Fluid Flow Vol. 17, 1996, 333-342.

[19] Le, A.-T., Coleman, GN, Kim, J. "Near-wall turbulence structures in three-dimensional boundary layer". International Journal Heat Fluid Flow, Vol. 21, 2000, 480-488.

[20] Wu, X., Squares, KD. "Large eddy simulation of an equilibrium three-dimensional turbulent boundary layer." AIAA J. Vol. 35, 1997, 67-74.

[21] El-Samni, OA, Yoon, HS, Chun, HH. "Direct numerical simulation of turbulent flow in a vertical channel with buoyancy orthogonal to the mean flow". Int. J. Heat Mass Transfer Vol. 48, 2005, 1267-1282.

[22] Iwamoto, K., Suzuki, Y., Kasagi, N. "Reynolds number effect on wall turbulence. toward effective feedback control". Int. J. Heat Fluid Flow, Vol. 23, 2002, 678-689.

[23] Kim, J., Moin, P., Moser, R. "Turbulence statistics in fully developed channel flow at low Reynolds number." J. Fluid Mech., Vol. 177, 1978, 133-166.

[24] Yoon, HS, El-Samni, OA, Chun, HH." Drag reduction in turbulent channel flow with periodically arrayed heating and cooling strips". Physics of Fluids Vol. 18, 2006, 025104.